UNIVERSITY OF LEEDS

This is a repository copy of *Wide-Area Identification of the Size and Location of Loss of Generation Events by Sparse PMUs*.

White Rose Research Online URL for this paper:
https://eprints.whiterose.ac.uk/169323/

Version: Accepted Version

---

**Article:**
Azizi, S orcid.org/0000-0002-9274-1177, Rezaei Jegarluei, M orcid.org/0000-0002-6770-7161, Salehi Dobakhshari, A et al. (2 more authors) (2020) Wide-Area Identification of the Size and Location of Loss of Generation Events by Sparse PMUs. IEEE Transactions on Power Delivery. ISSN 0885-8977

https://doi.org/10.1109/TPWRD.2020.3047228

---

© 2020 IEEE. Personal use of this material is permitted. Permission from IEEE must be obtained for all other uses, in any current or future media, including reprinting/republishing this material for advertising or promotional purposes, creating new collective works, for resale or redistribution to servers or lists, or reuse of any copyrighted component of this work in other works.

**Reuse**
Items deposited in White Rose Research Online are protected by copyright, with all rights reserved unless indicated otherwise. They may be downloaded and/or printed for private study, or other acts as permitted by national copyright laws. The publisher or other rights holders may allow further reproduction and re-use of the full text version. This is indicated by the licence information on the White Rose Research Online record for the item.

**Takedown**
If you consider content in White Rose Research Online to be in breach of UK law, please notify us by emailing eprints@whiterose.ac.uk including the URL of the record and the reason for the withdrawal request.

White Rose university consortium
Universities of Leeds, Sheffield & York

eprints@whiterose.ac.uk
https://eprints.whiterose.ac.uk/

# Wide-Area Identification of the Size and Location of Loss of Generation Events by Sparse PMUs

S. Azizi, *Senior Member, IEEE*, M. Rezaei Jegarluei, A. Salehi Dobakhshari, *Member, IEEE*,
G. Liu, *Student Member, IEEE*, and V. Terzija, *Fellow*, *IEEE*

***Abstract*—Timely identification of the size and location of loss of generation (LoG) events improves the effectiveness of remedial actions taken against this type of disturbances. This paper sets forth a novel method for LoG localization and size estimation by phasor measurements received in the control center within a reasonable wait time following the event inception. The bus impedance matrix is utilized to obtain a transfer function from the LoG location to variations of voltage and current phasors following the event. This results in an overdetermined system of linear equations whose closed-form solution provides the LoG location and size based upon the sum of squared residuals concept. The proposed method removes the need for the reception of specific measurements in the control center, and/or knowing the system inertia. This is in contrast with previous methods resorting to the swing equation of the center of inertia. The method lends itself to real-time applications for its robustness against partial communication network failures and losses of the time synchronization signal. Extensive simulations conducted on the IEEE 39-bus and 118-bus test systems verify the effectiveness and superiority of the proposed method over existing ones.**

***Index Terms*—Loss of generation, phasor measurement unit, underfrequency load shedding (UFLS), superimposed circuit.**

## I. Introduction

To meet legally-binding decarbonization commitments, many countries around the globe have set out ambitious targets for shifting towards a mostly-renewable generation mix in coming years. The inherent intermittency of renewable energies renders some important grid characteristics volatile, *i.e.*, to vary within an unprecedently wide range. This volatility is making assumptions of traditional operational, protection and control practices increasingly invalid. A recent outcome of this is the blackout in the UK on 9th August 2019 that left over one million people without electricity and disrupted public transport across the country [1]. This disturbance and other recent cascading failures call for revisiting current system integrity protection schemes [2].

Caused by sudden loss of generation (LoG) events, large active-power deficits are essentially counteracted by conducting underfrequency load shedding (UFLS). UFLS arrests further frequency decline by regaining the balance between generation and consumption in the system [3], [4]. This is conventionally accomplished by a trial-and-error process based upon a predetermined set of frequency thresholds. If local frequency measured by a UFLS relay falls below a certain frequency threshold, a prescribed amount of load will be shed by that relay [4]. Until the sum of load shed becomes sufficient, system frequency keeps declining and violating next frequency thresholds, thereby triggering the implementation of next steps of load shedding.

Variants of the conventional UFLS scheme are slow in nature and take much longer to deal with large LoG events, whilst the system is in more need of prompt remedial actions [5]. This is becoming quite problematic in systems with increasing renewable generation. The reason is that in contrast with conventional synchronous generators, renewable energy sources provide little or no inertia to the power system, reducing the system's stiffness against LoG events. This means the larger the share of renewable energy sources from the total generation is, the smaller the system inertia becomes. This may cause maximum frequency deviations to become unacceptably large. On the other hand, the volatility of system inertia makes it almost impossible to set conventional UFLS relays such that they function properly without overshedding or undershedding following LoG events under different operating conditions [2]. The sooner the size of an LoG event is determined, the more promptly the frequency decline can be arrested by shedding the same or even less amount of load in comparison with the conventional UFLS scheme.

To overcome the slowness of the conventional UFLS scheme, a number of adaptive methods have been proposed so far. The knowledge of the aggregate system inertia together with the rate of change of frequency (RoCoF) helps to estimate the size of the LoG event based on the center-of-inertia (CoI) concept [5-8]. The underlying assumptions of the swing equation model and using RoCoF measurements have been scrutinized in [6]. This reference discusses factors affecting the frequency response of the power system. With the proliferation of renewable energy sources, system inertia can hardly be assumed constant. In response, [9-12] estimate the system inertia based on phasor measurement unit (PMU) measurements. Another line of research in this area is focused on difficulties associated with the RoCoF measurement and how the measurement algorithm may affect the UFLS scheme in terms of demand not supplied [13], [14].

The wide-area frequency monitoring network, composed of a network of GPS-synchronized frequency disturbance recorders, uses local frequency measurements for localizing

Sadegh Azizi and Mohammad Rezaei Jegarluei are with the School of Electronic and Electrical Engineering, University of Leeds, Leeds LS2 9JT, UK (e-mail: s.azizi@leeds.ac.uk; elmrj@leeds.ac.uk).

Ahmad Salehi Dobakhshari is with the Faculty of Engineering, University of Guilan, Rasht 4199613776, Iran (e-mail:,salehi_ahmad@guilan.ac.ir).

Gaoyuan Liu and Vladimir Terzija are with the School of Electrical and Electronic Engineering, University of Manchester, Manchester M13 9PL, UK (e-mail: gaoyuan.liu@manchester.ac.uk; vladimir.terzija@manchester.ac.uk).

LoG events with an accuracy of 100 miles as well as reporting the event inception time [15], [16]. A similar approach is presented in [17] based on the arrival times of frequency waves recorded by PMUs. To avoid using RoCoF measurements, [18] utilizes synchronizing power coefficients to relate the change in active power of remaining generators to the generation imbalance in the system. Provided that PMUs installed at some generator terminals measure and transmit their active power outputs to the control center, the location and size of LoG events can be identified. Reference [19] presents an event location estimating process for power systems using PMU data supported by offline zonal analysis.

This paper proposes a different approach to identifying the location and size of LoG events using algebraic circuit equations. According to the theory of electric machinery, synchronous generators can each be modeled by a voltage source behind a sub-transient impedance for a few cycles following an event [20]. Thanks to the superimposed circuit concept detailed in Appendix A, a system of linear equations is derived based on sparse synchrophasor measurements to relate superimposed voltage and current phasors to the problem unknowns. Amongst the outage candidates, the one that best matches the collected measurements is identified as the true LoG event. The formulation proposed is also extended to enable its functioning with unsynchronized input phasors.

The salient features of the proposed method compared to previous research works can be summarized as follows:

- Leveraging the full potential of available synchrophasors without placing any constraints on PMU locations.
- No need of extensive offline simulation studies.
- Retaining the ability to localize and estimate the size of LoG events with unsynchronized input phasors.
- Facilitating effective UFLS for being fast and robust against communication failures.

The remainder of this paper is organized as follows. Section II proposes a linear formulation for the localization and size estimation of LoG events. The proposed formulation is then extended to account for temporary losses of the time synchronization signal. Performance evaluation is carried out in Section III through extensive simulation studies. Finally, the paper is concluded in Section IV.

## II. Proposed Method and Derivations

The proposed method for localization and size estimation of LoG events is detailed in this section. The bus impedance matrix of the grid, SCADA measurements of generator outputs and their internal impedances, as well as phasor measurements provided by PMUs are fed to the proposed method as inputs. The superimposed circuit concept, detailed in Appendix A, is used to build a linear system of equations for possible LoG events. The sum of squared residuals (*SoSR*) resulting from each candidate system of equations is deployed for pinpointing the location of the LoG event. The solution to the system of equations corresponding to the identified location is used to estimate the size of the event. The proposed formulation is then extended to be able to function properly with phasors that are not synchronized to a common time reference. This will be quite advantageous when the time-synchronization signal is temporarily lost.

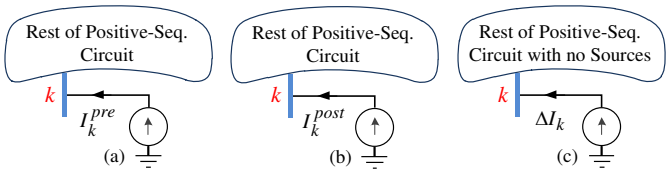


Fig. 1. (a) Pre-disturbance, (b) post-disturbance, and (c) superimposed positive-sequence circuits corresponding to an LoG event at bus k.

### A. Linear Systems of Equations Associated with LoG Events

Let us assume the LoG event is the trip of a number of generating units connected to bus $k$. Following this event, the current injection at this bus will change from $I_k^{pre}$ to $I_k^{post}$ as demonstrated in Figs 1(a) and 1(b). Resulting changes in voltages and currents of the rest of the power system can be associated to a hypothetical superimposed circuit with only one current injection at the bus $k$ as shown in Fig. 1(c). The value of this current source will be equal to $\Delta I_k = I_k^{post} - I_k^{pre}$. Let $\Delta V_i$ and $\Delta J_{uv}$ represent the positive-sequence superimposed voltage at bus $i$ and sending-end superimposed current of line $u$-$v$, respectively. As explained in Appendix A, one can write for this superimposed circuit

$$\Delta V_i = Z_{i,k}\Delta I_k \tag{1}$$

$$\Delta J_{uv} = C_{uv,k}\Delta I_k \tag{2}$$

where $Z_{i,k}$ represents the element in the $i$-th row and $k$-th column of the bus impedance matrix of the positive-sequence circuit, denoted by $\boldsymbol{Z}$. The generating units connected to bus $k$ are not taken into account whilst building the bus impedance matrix as they are entirely represented by a current source injecting different amounts of current before and after the LoG inception. Other generators in the system are each modeled by a sub-transient reactance in series with a constant voltage source. The values of these voltage sources are not needed for our calculations as they do not appear in the superimposed circuit [21]. The Thevenin-Norton equivalent theorem is used to transform this model into a constant current source in parallel with the corresponding reactance [22].

Let us assume $n$ equations can be derived from PMU data in the form of (1) or (2), which together result in a system of linear equations as follows

$$\boldsymbol{m} = \boldsymbol{h}\Delta I_k + \boldsymbol{\varepsilon} \tag{3}$$

where $\boldsymbol{m}$ is the vector of superimposed measurements and $\boldsymbol{h}$ is the coefficient vector. Besides, the vector $\boldsymbol{\varepsilon}$ represents measurement errors. This system of equations can be readily solved using the weighted least-squares (WLS) method. Let $\boldsymbol{R}$ denote the covariance matrix of measurement errors, which is an $n$-by-$n$ diagonal matrix whose $i$-th non-zero entry is the variance of the $i$-th measurement, *i.e.*, $\sigma_i^2$. The closed-form solution of (3) can be obtained by the WLS method as below

$$\Delta\hat{I}_k = \sum_{i=1}^{n}\frac{h_i^* m_i}{\sigma_i^2} \Bigg/ \sum_{i=1}^{n}\frac{|h_i|^2}{\sigma_i^2} \tag{4}$$

where $(.)^*$ refers to the conjugate transpose of the argument. The hat sign is used to emphasize that the solution would not be exactly equal to the true value owing to measurement

errors, but will be an estimate. The WLS method approximates the solution of the overdetermined system of equations by minimizing the sum of the squares of the residuals made in the equations [23]. In other words, (4) is the outcome of the following minimization problem:

$$\text{Min} \quad SoSR=\left[\boldsymbol{m}-\boldsymbol{h}\Delta\hat{I}_k\right]^{*}\boldsymbol{R}^{-1}\left[\boldsymbol{m}-\boldsymbol{h}\Delta\hat{I}_k\right] \tag{5}$$

Equation (4) provides the sudden current injection change caused by the LoG event based on the available superimposed current and voltage measurements provided by PMUs.

### *B. LoG Event Localization and Size Estimation*

This paper is aimed at identifying the location and size of the LoG event. The formulation derived in the previous subsection is applicable only if the LoG event location is known a-priori. Nonetheless, this is essentially one of the unknowns to be determined. Our assumption here is that the nodal current injection and active power injection at bus $k$ prior to the event inception, respectively denoted by $I_k^{pre}$ and $P_k^{pre}$, are known to the control center by the SCADA system. The LoG event size, denoted by $\Delta P$, would be equal to or smaller than $P_k^{pre}$, considering the possibility of partial outages of generating units connected to bus $k$.

Let us assume the system of equations corresponding to the true LoG event is built and solved. If measurements are ideal, and hence the developed equations are error-free, the *SoSR* obtained will be exactly zero. The *SoSR* of other candidate locations would take non-negligible values since the corresponding equations do not hold, as justified in Appendix B. In order to localize the LoG event, thus, (3) should be built for every candidate LoG location and the corresponding *SoSR* needs to be calculated. The smallest *SoSR* obtained is taken as the indicator of the LoG location. Mathematically speaking, this can be expressed in the following format

$$k = Arg\left\{\underset{q\in\boldsymbol{G}}{\text{Min}} \quad SoSR=\left[\boldsymbol{m}-\boldsymbol{h}\Delta\hat{I}_q\right]^{*}\boldsymbol{R}^{-1}\left[\boldsymbol{m}-\boldsymbol{h}\Delta\hat{I}_q\right]\right\} \tag{6}$$

where $\boldsymbol{G}$ is the set of all candidate LoG locations. As shown in Appendix C, there is a closed-form solution for *SoSR* at each candidate location.

After the event location is identified, *e.g.*, bus $k$, the sudden current injection change at bus $k$ resulting from this event is calculated from (4). Without loss of generality, it is assumed that the $u$ parallel generating units connected to bus $k$ are identical. The event is assumed to be the outage of some or all of the generating units at this location. As will be justified in Appendix D, $\Delta P$ caused by this LoG event can be estimated from the following formula

$$\Delta P = \left|\frac{uZ_{k,k}+X_k''}{uZ_{k,k}+X_k''\alpha^{-1}}\right| P_k^{pre} \tag{7}$$

where $\alpha$ is the ratio between $|\Delta\hat{I}_k|$ and $|I_k^{pre}|$. The former is given by (4) and the latter is assumed to be known thanks to the SCADA system. Besides, $X_k''$ is the reactance of each generating unit connected to bus $k$. In the case of the outage of all units, $\alpha$ will be equal to unity, which makes the LoG size obtained from (7) equal to $P_k^{pre}$, as expected. A flowchart of the proposed method is shown in Fig. 2. It can be seen that the real-time calculations are limited to the evaluation of *SoSR* for candidate locations and identification of the event size. Event detection in this paper is carried out based on the RoCoF exceeding a predetermined threshold, i.e. 0.05 Hz/s. More advanced techniques such as that of [10] can be used, if higher accuracy is needed.

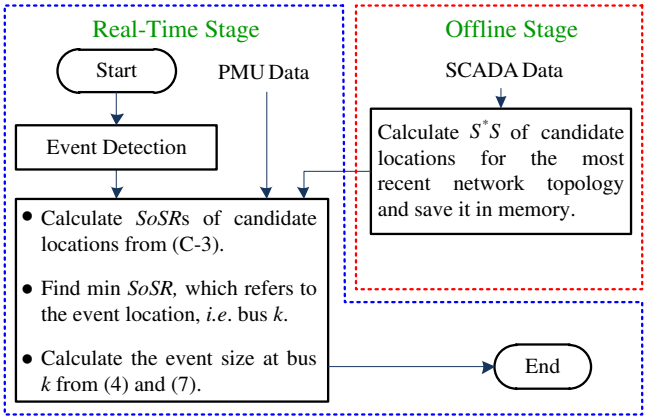

Fig. 2. Flowchart of the proposed method.

### *C. Loss of the Time-Synchronization Signal*

The system of linear equations (3) is built based upon the assumption that phasors collected by PMUs are all synchronized to a common time reference. Therefore, a temporary loss of the time-synchronization signal will render this system unsolvable. It should be noted that voltage and current phasors calculated by a PMU in a substation will be all synchronized to the local time reference of that PMU [24]. The phase-angles of phasors associated with a PMU remain extremely accurate with respect to each other within the time frame of interest to LoG event localization [24], [25].

In the case of a temporary loss of the time synchronization signal, the measurement vector needs to be modified to account for different time references of PMUs. Let us assume there are $s$ PMUs in the system and $\boldsymbol{m}_{p1}$, $\boldsymbol{m}_{p2}$, … , $\boldsymbol{m}_{ps}$ are vectors representing the measurements provided by $PMU_1$ to $PMU_s$, respectively. Without loss of generality, let the reference phase-angle of bus 1 be taken as the common reference for the whole grid. By defining the unknown synchronization operators $e^{j\delta_2},\ldots.e^{j\delta_s}$ for measurements provided by $PMU_2$ to $PMU_s$, (3) changes to

$$\begin{bmatrix}\boldsymbol{m}_{p1}\\ e^{j\delta_2}\boldsymbol{m}_{p2}\\ \vdots\\ e^{j\delta_s}\boldsymbol{m}_{ps}\end{bmatrix}=\begin{bmatrix}h_1\\ \vdots\\ h_n\end{bmatrix}\Delta I_k+\begin{bmatrix}\varepsilon_1\\ \vdots\\ \varepsilon_n\end{bmatrix} \tag{8}$$

The system of equations (8) is nonlinear in terms of $\Delta I_k$ and synchronization angles $\delta_2,\cdots,\delta_s$. The solution of (8) demands iterative solving processes, which would not only be computationally expensive but also prone to divergence and the multiplicity of solution.

To remove the foregoing concerns, the synchronization operators $e^{j\delta_2},\ldots.e^{j\delta_s}$ are treated as problem unknowns,

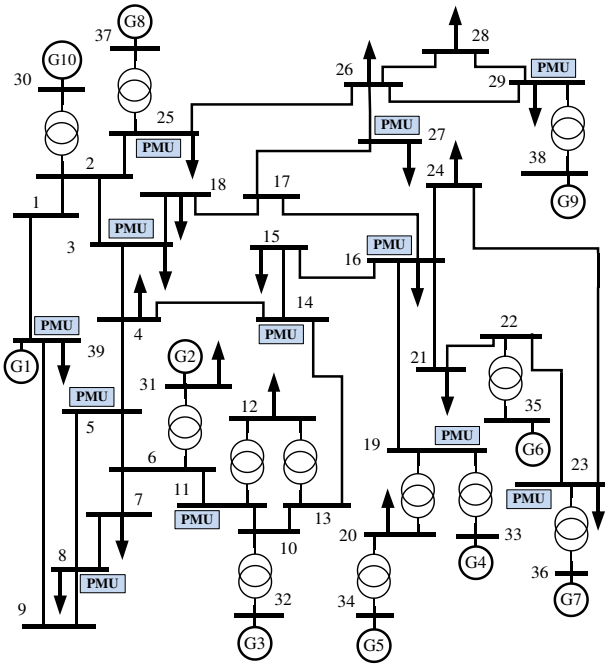


Fig. 3. Single-line diagram of the IEEE 39-bus test system.

instead of synchronization angles. This change of variable technique helps to maintain the linearity of the equations in (8), hence eases the solution process, as below

$$\begin{bmatrix} \boldsymbol{m}_{p1} \\ 0 \\ \vdots \\ 0 \end{bmatrix} = \begin{bmatrix} \begin{bmatrix} h_1 \\ h_2 \\ \vdots \\ h_{n-1} \\ h_n \end{bmatrix} & [0] & [0] & \cdots & [0] \\ & -\boldsymbol{m}_{p2} & [0] & \cdots & [0] \\ & [0] & -\boldsymbol{m}_{p3} & \cdots & [0] \\ & \vdots & \vdots & \ddots & \vdots \\ & [0] & [0] & \cdots & -\boldsymbol{m}_{ps} \end{bmatrix} \begin{bmatrix} \Delta I_k \\ e^{j\delta_2} \\ \vdots \\ e^{j\delta_s} \end{bmatrix} + \boldsymbol{\varepsilon} \quad (9)$$

The foregoing rearrangement yields a system of linear equations for the synchronization operators and superimposed current at bus $k$. This system can be readily solved by the WLS method to obtain the values of unknown synchronization angles and the superimposed current of the lost generating units. The rest of LoG localization and size estimation process remains the same as that with synchronized measurements.

## III. Performance Evaluation

The performance of the proposed method for localization and size estimation of LoG events is evaluated by conducting extensive simulations on the IEEE 39-bus and 118-bus test systems [26]. A general performance evaluation with both synchronized and unsynchronized measurements is presented first. The impact of unsynchronized measurements is studied in the next step. The sensitivity of the proposed method to topology, line parameter and measurement errors is also scrutinized. Then, the impact of different number/locations of PMUs is examined. Finally, the performance of the proposed method is compared with that of similar methods.

Simulations are carried out in DIgSILENT PowerFactory and voltage and current waveforms recorded are filtered using an anti-aliasing Butterworth filter with a cut-off frequency of 400 Hz. Then, they are sampled with a sampling frequency of 2 kHz. The discrete Fourier transform (DFT) is used to estimate phasors of recorded time-domain waveforms. Any other phasor estimation methods that provide more accurate phasors could be used to offer more accuracy, if needed. Without loss of generality, the variance of all measurements is considered to be the same. In regard to the phasor estimation process, the estimated size becomes accurate after a full data window length passes from the LoG inception [4]. The estimated value from this time instant is averaged for one power-frequency cycle and is reported as the LoG size.

TABLE I
*SoSR*s of Candidate Locations Following the Outage of G3

| SoSR | G1 | G2 | G3 | G4 | G5 | G6 | G7 | G8 | G9 | G10 |
|---|---|---|---|---|---|---|---|---|---|---|
| Abs. | 49.6 | 53.8 | 0.01 | 53.8 | 54.5 | 54.7 | 54.5 | 54.1 | 54.5 | 54.37 |
| Norm. | 0.91 | 0.98 | ~0 | 0.98 | 0.99 | 1 | 0.99 | 0.98 | 0.99 | 0.99 |

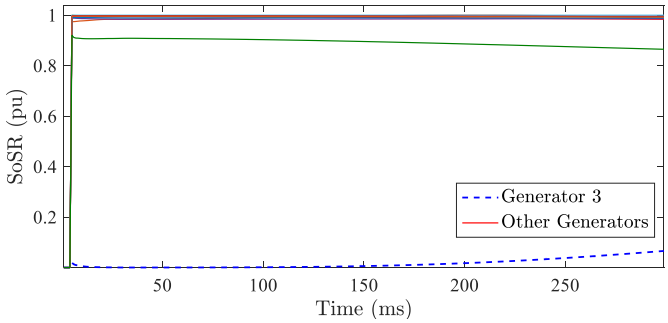


Fig. 4. *SoSRs* of different candidate LoG locations calculated over time following the outage of all generating units connected to bus 32.

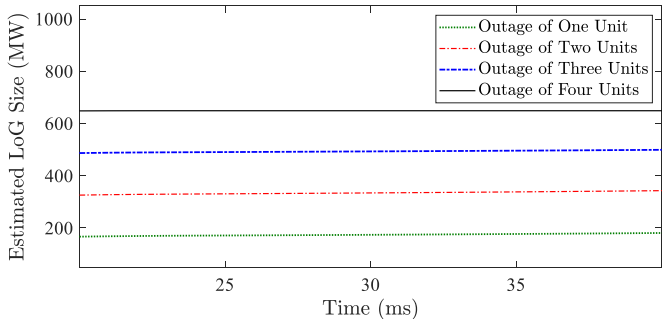


Fig. 5. Estimated size of the LoG event following the outage of different numbers of the generating units connected to bus 32.

### A. General Evaluation of the Proposed Method

LoG localization and size estimation by the proposed method are demonstrated using arbitrarily selected examples. As shown in Fig. 3, buses 3, 5, 8, 11, 14, 16, 19, 23, 25, 27, 29 and 39 are equipped with PMUs in the IEEE 39-bus test system [26]. Four generating units are connected to bus 32 with total active power injection of 650 MW and are tripped at $t = 0$ sec. To normalize the *SoSR*s of these candidate LoG locations, each *SoSR* at any time instant is divided by the maximum *SoSR* amongst all *SoSR*s calculated at that time instant. The absolute and normalized *SoSRs* calculated for candidate LoG locations at 50 milliseconds following the LoG event are listed in Table I. Fig. 4 demonstrates the normalized *SoSRs* for up to 300 milliseconds after the LoG event. As can be seen, the smallest *SoSR* correctly indicates the true LoG location with enough distinction from other candidate LoG

TABLE II
LOG SIZE ESTIMATION ERRORS ON THE IEEE 39-BUS TEST SYSTEM

| Scenario | Size Estimation Error (%) | | | | | | | | | |
|---|---|---|---|---|---|---|---|---|---|---|
| | G1 | G2 | G3 | G4 | G5 | G6 | G7 | G8 | G9 | G10 |
| Base-case | 0.84 | 0.13 | 0.24 | 1.71 | 0.01 | 0.12 | 0.33 | 0.28 | 0.11 | 1.74 |
| Light-loading | 0.12 | 1.08 | 0.68 | 1.59 | 0.87 | 0.84 | 0.69 | 0.24 | 0.80 | 1.93 |
| Heavy-loading | 0.22 | 0.07 | 0.24 | 1.81 | 0.08 | 0.52 | 0.61 | 0.35 | 0.10 | 1.98 |

TABLE III
LOG SIZE ESTIMATION ERRORS ON THE IEEE 118-BUS TEST SYSTEM

| Size Estimation Error (%) | | | | | | | | | |
|---|---|---|---|---|---|---|---|---|---|
| G1 | G2 | G3 | G4 | G5 | G6 | G7 | G8 | G9 | G10 |
| 0.04 | 1.86 | 3.19 | 1.78 | 1.38 | 1.20 | 0.20 | 0.21 | 3.10 | 1.59 |

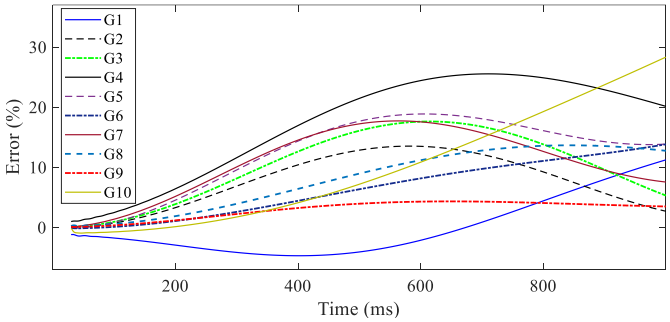


Fig. 6. Size estimation error over time for LoG events at different locations.

locations. Extensive simulations conducted confirm that the *SoSR* index proposed for pinpointing the LoG event location remains highly reliable for up to one second or even longer following the LoG event inception. This guarantees that there will be enough time to locate the tripped generator. The estimated LoG sizes over time for different LoG events at the foregoing location are demonstrated in Fig. 5.

For a thorough evaluation of the proposed method, different LoG events at G1 to G10 are examined. In addition to the base-case loading scenario, heavy- and light-loading scenarios are also created for the IEEE 39-bus test system by uniformly changing the amount of generation/load in the system by ±50%. This is to study the effect of system loading on the performance of the proposed method, as well. Following each LoG event, the *SoSR* is calculated for all candidate LoG locations. The smallest *SoSR* is sought to infer the true LoG location and proceed with its size estimation. Event localization is successfully carried out for the entire simulations in all scenarios. LoG size estimation results for 50 milliseconds after LoG event are summarized in Table II. As can be seen, size estimation errors do not exceed 2% of the true LoG size in any of cases. This justifies that loading condition has an insignificant impact on the accuracy and success rate of the proposed method. Fig. 6. shows the error of LoG size estimation at different locations for up to 1 sec following the event inception. The size of estimation error increases as the time progresses, as expected. Therefore, the decision should be made based on the initial data samples received if we are to achieve a higher level of accuracy.

The proposed method is also tested on the IEEE 118-bus test system with 28 PMUs [27]. LoG event localization is successfully carried out in all cases. Estimation results following the outage of 10 arbitrarily selected generators

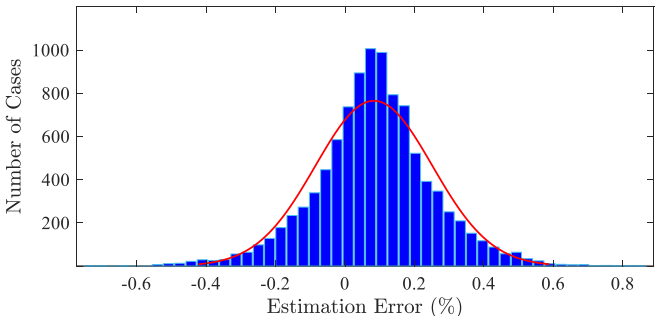


Fig. 7. Estimated LoG size with unsynchronized measurements following the outage of all generating units at bus 33.

TABLE IV
LOG SIZE ESTIMATION WITH UNSYNCHRONIZED PHASORS

| Tripped Generator | G1 | G2 | G3 | G4 | G5 | G6 | G7 | G8 | G9 | G10 |
|---|---|---|---|---|---|---|---|---|---|---|
| Ave. Error (%) | 0.18 | 0.93 | 0.15 | 0.14 | 0.56 | 1.22 | 0.27 | 0.15 | 0.14 | 0.90 |
| Max. Error (%) | 0.91 | 1.55 | 0.86 | 1.88 | 1.27 | 1.77 | 0.92 | 0.72 | 0.72 | 1.96 |

connected to buses 10, 25, 26, 49, 65, 66, 69, 80, 89, and 100 are summarized in Table III.

The evaluation of the scalar index *SoSR* for each candidate location will incur a limited number of multiplication and addition operations as shown in Appendix C. The computation time of the whole procedure for the IEEE 39-bus test system with 48 measurements and 10 generators is about 0.1 ms, on a 2.8 GHz processor with 8 GB of RAM. This for the IEEE 118-bus test system with 141 measurements and 19 generators is around 0.4 ms. For a large power system with 500 phasor measurements, calculating *SoSR* for each candidate location will take no more than 0.2 ms. This will amount to a total of 20 ms for the whole procedure if the system has 100 generator buses, which is quite acceptable from a practical point of view. More importantly, the evaluation of *SoSR*s are totally independent of each other, and if needed, the related process could be highly parallelized on both software and hardware levels. On the other hand, the LoG identification can be easily limited to the disturbed area if the boundaries of that area are observed by PMUs. The same approach has been already introduced and successfully tested by the authors in [21].

### *B. Performance with Unsynchronized Input Phasors*

The ability of the proposed method in functioning with unsynchronized phasors is examined in this subsection. First, all estimated phasors are multiplied by a random number accounting for a total vector error (TVE) of 1%, where TVE is a measure of the difference between the phasor estimated and the true phasor itself [29]. To make these non-ideal phasors unsynchronized, voltage and current phasors associated to each PMU are multiplied by a random complex number with a magnitude of one and a phase-angle between 0 and 2π.

Results obtained demonstrate that LoG localization and size estimation can be successfully accomplished even with unsynchronized inputs. As an example, simulations are repeated 10,000 times for an LoG event at bus 33. The event size is calculated in each case and results obtained are summarized in Fig. 7. As can be seen, size estimation is successfully accomplished with an average error of 0.15% and

TABLE V
LOG SIZE ESTIMATION SENSITIVITY TO TOPOLOGY ERRORS

| Transmission Line/Transformer Index | Size Estimation Error (%) | | | |
|---|---|---|---|---|
| | Ave. | Max. | Ave. | Max |
| | Not considered while in service | | Considered while not in service | |
| 17-18 | 2.13 | 9.85 | 0.68 | 1.94 |
| 26-28 | 1.70 | 10.00 | 0.52 | 1.29 |
| 11-12 | 0.68 | 1.85 | 0.95 | 4.23 |

TABLE VI
LOG SIZE ESTIMATION SENSITIVITY TO LINE PARAMETER ERRORS

| Results | Variation Range of Line Parameter Errors (%) | | | | | | | | | |
|---|---|---|---|---|---|---|---|---|---|---|
| | ±1 | ±2 | ±3 | ±4 | ±5 | ±6 | ±7 | ±8 | ±9 | ±10 |
| Ave. Err. | 0.56 | 0.57 | 0.57 | 0.58 | 0.60 | 0.62 | 0.64 | 0.65 | 0.68 | 0.71 |
| Max. Err. | 2.04 | 2.19 | 2.40 | 2.53 | 2.72 | 3.02 | 3.42 | 3.42 | 4.89 | 4.60 |

TABLE VII
LOG SIZE ESTIMATION SENSITIVITY TO GENERATOR PARAMETER ERRORS

| Results | Variation Range of Generator Parameter Errors (%) | | | | | | | | | |
|---|---|---|---|---|---|---|---|---|---|---|
| | ±5 | ±10 | ±15 | ±20 | ±25 | ±30 | ±35 | ±40 | ±45 | ±50 |
| Ave. Err. | 0.46 | 0.46 | 0.46 | 0.47 | 0.47 | 0.47 | 0.47 | 0.47 | 0.48 | 0.48 |
| Max. Err. | 1.74 | 1.75 | 1.79 | 1.83 | 1.84 | 1.87 | 1.90 | 1.94 | 1.96 | 1.98 |

TABLE VIII
SENSITIVITY OF LOG SIZE ESTIMATION TO MEASUREMENT ERRORS

| Results | Variation Range of Measurement Errors (%) | | | | | | | | | |
|---|---|---|---|---|---|---|---|---|---|---|
| | ±1 | ±2 | ±3 | ±4 | ±5 | ±6 | ±7 | ±8 | ±9 | ±10 |
| Ave. Err. | 0.58 | 0.61 | 0.67 | 0.72 | 0.79 | 0.85 | 0.92 | 0.98 | 1.07 | 1.12 |
| Max. Err. | 2.27 | 2.70 | 3.20 | 3.70 | 4.60 | 5.18 | 5.11 | 5.15 | 6.70 | 7.18 |

a standard deviation of 0.2%. To be more inclusive, extensive simulations are carried out on the IEEE 39-bus test system in the base-case loading scenario for different LoG locations. Size estimation using unsynchronized phasors are performed and obtained results are summarized in Table IV. It can be observed that the accuracy achieved is quite comparable to that with synchronized input phasors.

### C. Impact of Topology, Parameter and Measurement Errors

In this subsection, the impact of topology, parameter, and measurement errors on the success rate of localization and accuracy of size estimation is scrutinized. Regarding topology errors, a single transmission line/transformer is either considered while not actually in service or not considered while actually in service. To show how much this could affect the accuracy of the proposed method, three transmission lines/transformers are considered. Table V demonstrates the maximum and average errors caused by these topology inaccuracies in LoG size estimation. Simulations show that the error of size estimation will not exceed 10% of the true LoG size as long as the topology error results from the status of one series element. Even in this condition, the event location is carried out successfully in all simulated cases.

Extensive simulations are conducted here to study the effect of transmission line and generator parameter errors on the success rate of the proposed method. Tables VI and VII summarize results obtained when lines/generators are considered to have random parameter errors within different ranges. Each simulated case is repeated 1,000 times for reporting average and maximum size estimation errors. For line/generator parameter errors of up to 10%, the proposed method remains successful in LoG event localization. As expected, the estimation error increases as the variation range of parameter errors is widened.

TABLE IX
SENSITIVITY OF LOG SIZE ESTIMATION TO THE NUMBER OF PMUS

| IEEE 39-Bus Test System | | | | | | | | | |
|---|---|---|---|---|---|---|---|---|---|
| No. of PMUs | 12 | 11 | 10 | 9 | 8 | 7 | 6 | 5 | 4 |
| Ave. Err. (%) | 0.60 | 0.66 | 0.86 | 0.88 | 1.02 | 1.11 | 1.33 | 1.47 | 1.55 |
| IEEE 118-Bus Test System | | | | | | | | | |
| No. of PMUs | 28 | 26 | 24 | 22 | 20 | 18 | 16 | 14 | 12 |
| Ave. Err. (%) | 1.60 | 1.62 | 1.71 | 1.72 | 1.79 | 1.82 | 1.83 | 1.93 | 1.99 |

The success rate of the proposed method is also dependent on measurement errors, similar to that of any other methods. This is studied here by using measurement errors of different TVEs, with normal distribution around the true value of corresponding phasors. Table VIII reports obtained results where the three-sigma criterion is employed for reporting the error range. As expected, larger measurement errors result in less accuracy in LoG size estimation. From a practical point of view, the proposed method proves to have sufficient robustness against different sources of inaccuracies. Providing the size and the location of the LoG event, it can help system operators to take proper remedial actions as fast as possible.

An accurate impedance matrix is a prerequisite for the proposed method to guarantee a highly reliable performance. One data sample after the event inception will be enough to this end. Next events such as sympathetic tripping of Distributed Generators (DGs) will not affect the performance of the proposed method, as it takes several power-frequency cycles for any component to sense the incident and respond to it by disconnecting from the rest of the grid. If prior to the LoG event a disturbance changes the network topology, this change must be fed to the method, as otherwise, errors in LoG localization/size estimation will be inevitable. A special case is when a line/transformer trip results in the disconnection of a generator from the rest of the system. In this case, the proposed method will correctly pinpoint that generator as the line/transformer outage and the generator outage seem the same from the rest of the system. However, if the line trip is somewhere else in the system, this will adversely affect the accuracy of the proposed method to some extent. The proposed method is based on the approximation of the internal reactance of non-tripped generators by their sub-transient reactance. This introduces some errors into the estimated LoG size over time as shown in Fig. 6. If the surrounding area of generators is not covered by PMUs, the LoG size estimation might incur larger errors.

### D. Observability and PMU Coverage

Observability is not a prerequisite for using the proposed method, and the *SoSR* index is capable of pinpointing the event location by the measurements of any two PMUs or more as justified in Appendix B. To demonstrate this, the proposed method is applied with different numbers of PMUs. For each specific number of PMUs, 100 randomly created placements

TABLE X
LOG LOCALIZATION AND SIZE ESTIMATION BY DIFFERENT METHODS

| Reference | [8] | [15] [16] | [17] | [18] | [19] | Prop. |
|---|---|---|---|---|---|---|
| Need offline studies? | No | No | Yes | No | Yes | No |
| Specific sensor locations? | Yes | No | Yes | Yes | Yes | No |
| Need Time-Synch Signal? | Yes | Yes | Yes | Yes | Yes | No |
| Tolerate Sensor Losses? | No | Yes | No | Yes | Yes | Yes |
| Estimate both size and location? | No | Yes | No | Yes | No | Yes |
| Computational burden: | Low | Low | High | High | High | Low |

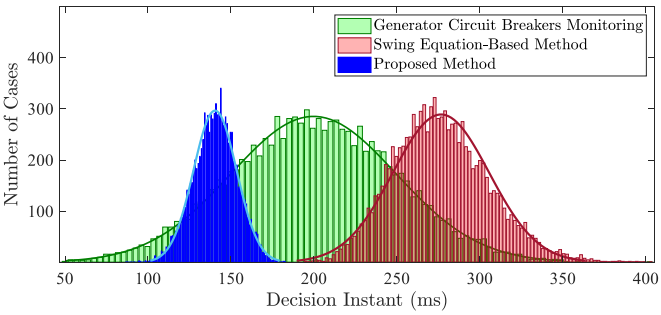


Fig. 8. Comparison between the proposed, direct GCB monitoring and swing equation-based LoG size estimation methods in terms of execution time.

have been considered. LoG localization has been successfully accomplished in all simulations regardless of the number and locations of PMUs. The average size estimation errors obtained is summarized in Table IX. As can be seen, results are all acceptable from a practical point of view, while the number and locations of PMUs are not constrained by the proposed method.

The variance of the estimated superimposed current by (4) can be obtained from [28]:

$$\mathrm{Var}(\Delta\hat{I}_k) = \left[\boldsymbol{h}^* \boldsymbol{R}^{-1} \boldsymbol{h}\right]^{-1} \tag{10}$$

This means better accuracy will be achieved with a greater number of PMUs. Simulations also suggest that there is a correlation between the PMU coverage in the proximity of the true LoG event and the *SoSR* of other candidate locations. The more intensely PMUs cover the true LoG location, the bigger the *SoSRs* calculated for other candidate locations are.

### *E. Comparison with Other LoG Size Estimation Methods*

The most trivial approach to LoG localization is the direct monitoring of all generator circuit breakers (GCBs) to detect their outages. The size of LoG can be then identified from SCADA information from right before the LoG event. Nonetheless, this cannot be considered a flawless solution as transmitting the corresponding signals is inevitably subject to indefinite communication latencies and even complete failure. Therefore, there have been several approaches aimed at LoG size estimation based on additional useful information offered by the wide-area monitoring system [30]. Table X compares the proposed method with other existing methods from different perspectives. As can be seen, a majority of existing methods require synchrophasors and would consequently suffer from time-synchronization issues. While the proposed method is able to function with any set of data, some other methods put demanding constraints on the number and locations of PMUs, and might even require extensive offline simulation studies raising accuracy and computational burden concerns. The developed system of equations is linear, which means bad data detection/identification approaches such as the normalized residual test can be readily deployed to overcome the inclusion of bad data in the measurement set [23].

A large number of simulations are carried out in this subsection to compare the proposed LoG size estimation method with the direct GCB monitoring and swing equation-based methods in terms of speed. According to IEEE Std. C37.118.2 [31], system-wide communication latencies are not definite. Aggregated communication latencies are supposed to have a normal distribution with mean 200 ms and standard deviation 50 ms in this study. Besides, it is assumed that all buses in the system are equipped with PMUs. A total of 10,000 Monte Carlo simulations are carried out in order to draw solid conclusions from obtained results. While the swing equation-based method must wait for the receptions of all generator frequencies before proceeding with calculations, the proposed method is set to operate once the post-event data of five PMUs are received in the control center. The direct GCB monitoring method determines the size and location of the LoG event upon the reception of the PMU data demonstrating that the active power output of the tripped generator has dropped to zero.

Fig. 8 demonstrates the distributions of decision time instants by different methods from the event inception to determining the LoG size. The average decision time by the proposed, direct GCB monitoring and swing equation-based methods are 140 ms, 200 ms, 275 ms, respectively. The superiority of the proposed method over the swing equation-based method can be easily verified from this figure. The reason for this superiority is that the swing equation-based method needs all measurements to be received, contrary to the former. Although the direct GCB monitoring method is faster than the proposed method in 12.5% of cases, it would need more time to function when the measurement associated to the tripped generator is delayed. Not being reliant on any specific measurements, the proposed method would act upon a limited number of measurements received early enough, thus taking less time to come up with a decision. Employing the proposed method together with direct GCB monitoring could reduce the average decision time to 135 ms.

### *F. Applications in Underfrequency Load Shedding*

The proposed method is not a novel UFLS scheme, but a method for wide-area monitoring of LoG events with no specific constraints over measurement locations/number. Centralized UFLS is just used as an example here to show how timely identification of LoG events can improve the performance of emerging centralized UFLS methods. Indeed, fast estimation of the size of LoG events is quite advantageous to counteracting their impact by shedding an appropriate amount of load at a right time and right locations. In this subsection, the performance of the conventional UFLS scheme is compared with a UFLS scheme designed based on the proposed LoG size estimation method. The conventional UFLS scheme is set to shed 7.5% of the total system load each time frequency violates the frequency thresholds 49.5, 49.2, 49, and 48.8 Hz [2]. The proposed UFLS relays are set to shed the designated load once frequency measured by the relay

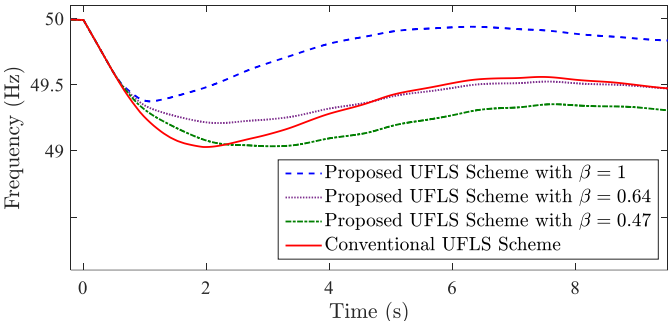


Fig. 9. Frequency response after UFLS with different adjustment coefficients.

falls below 49.5 Hz. It is well established that the amount of load shed by the conventional UFLS scheme following an LoG event is normally smaller than the event size [2]. To offer this flexibility, a less-than-unity adjustment coefficient $\beta$ is multiplied by the LoG size estimated by the proposed method to have UFLS relays compensate for a predefined portion of the generation imbalance caused by the LoG event.

Fig. 9 shows the frequency response of the center of inertia of the system following a 1600-MW LoG event whilst the total system inertia is reduced to 2.6 sec. The conventional scheme sheds 64% of the event size. By setting $\beta$=0.64 pu, the proposed UFLS scheme will also shed the same amount of load while reducing the maximum frequency deviation by 0.2 Hz compared to the former. The same maximum frequency deviation will be achieved by both schemes if $\beta$ is set to 0.47 pu. Nonetheless, the load shed by the proposed scheme will be only 74% of that by the conventional scheme. For $\beta$=1 pu, the proposed scheme sheds an amount of load equal to the LoG size, which reduces the maximum frequency deviation by 0.35 Hz compared to that by the conventional UFLS scheme. These responses demonstrate the flexibility that can be gained by the fast estimation of the LoG size using the proposed method.

If the monitoring of GCBs is the only tool deployed for LoG detection, we will be left with no alternative measures in the case of failure of the corresponding measurement device/communication channel, or even unacceptably long delays of system-wide communication [31]. This does not apply to the proposed method as it is not reliant on any single measurement. Besides, the 200 ms improvement offered by the method will be extremely beneficial to the remedial actions taken against LoG events with large RoCoFs, e.g. greater than 1 Hz/s. The extra computation burden can be seen as the price paid for improving frequency performance by leveraging the data of PMUs already installed in the system.

## IV. Conclusion

This paper proposes a new approach for localization and size estimation of loss of generation (LoG) events, based upon a limited number of phasor measurements recorded within a few power-frequency cycles following the event inception. Taking advantage of the bus impedance matrix, delayed or missing data of any PMU would be tolerable without affecting the method's performance. This is the case while existing methods require a predetermined set of measurements in order to function properly, which is a major drawback knowing that the latency of system-wide communication is neither definite nor predictable. On the other hand, the proposed method does not require any offline simulation studies, which makes its deployment relatively straightforward. The input phasors to the proposed method do not need to be necessarily synchronized, guaranteeing the robustness against temporary losses of the time synchronization signal.

Employing the proposed method in parallel with the direct monitoring of generator circuit breakers can effectively limit the decision time to a couple of hundreds of milliseconds following the LoG event inception. The linearity of the formulation developed makes the corresponding solving process much faster than that of existing formulations requiring iterative solving processes. Thanks to its robustness against the foregoing technical challenges, the proposed method lends itself to effective underfrequency load shedding in modern power systems with highly reduced inertia. The proposed method can also be employed for monitoring the sudden addition or disconnection of shunt elements (e.g. loads) to/from the system.

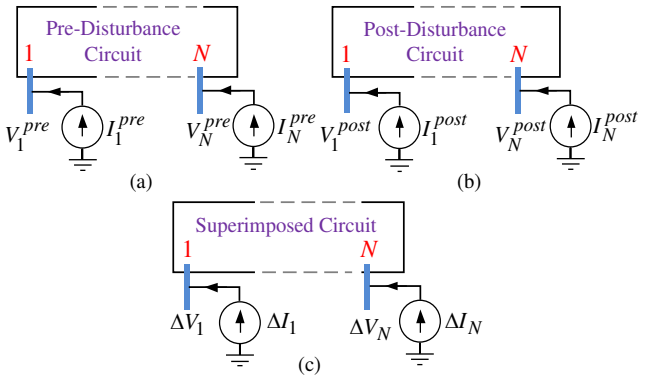


Fig. A1. (a) Pre-disturbance, (b) Post-disturbance and (c) Superimposed circuits for a disturbance which is sudden changes of nodal current injections.

## Appendix A: Superimposed Circuit Derivations

The disturbance of interest is defined as sudden changes in nodal current injections in the circuit. Figs A1(a) and A1(b) show the corresponding pre- and post-disturbance circuits with the same topology, but with nodal current sources of different values. Possessing the same topology and elements, these two circuits have the same bus impedance matrix denoted by $\boldsymbol{Z}$. The circuit nodes in Fig. A1 are indexed 1 to $N$. If $\boldsymbol{V}^{pre}$ and $\boldsymbol{V}^{post}$ denote the vector of node voltages respectively before and after the disturbance, the nodal equations for the two circuits can be written as [22]:

$$\boldsymbol{V}^{pre} = \boldsymbol{Z}\boldsymbol{I}^{pre} \tag{A-1}$$

$$\boldsymbol{V}^{post} = \boldsymbol{Z}\boldsymbol{I}^{post} \tag{A-2}$$

where, $\boldsymbol{I}^{pre}$ and $\boldsymbol{I}^{post}$ are the vectors of nodal currents, before and after the disturbance, respectively. By subtracting (A-1) from (A-2) one obtains

$$\Delta\boldsymbol{V} = \boldsymbol{Z}\Delta\boldsymbol{I} \tag{A-3}$$

Equation (A-3) resembles the nodal equations of a circuit and can be attributed to a hypothetical, so-called superimposed circuit (see Fig. A1(c)). Node voltages, branch currents and nodal currents of the superimposed circuit are equal to the differences between their corresponding quantities before and after the disturbance. This explains why

voltage and current quantities in the superimposed circuit are all indicated by the Δ symbol.

The letters *I* and *J* are used in this paper to denote nodal current injections and branch currents, respectively. Let $Z_{i,j}$ denote the element in the *i*-th row and *j*-th column of the bus impedance matrix of a superimposed circuit with *N* nodes. If $\Delta I_j$ refers to the superimposed nodal injection at a node *j*, the superimposed voltage at any node *i* can be obtained from

$$\Delta V_i = \sum_{j=1}^{N} Z_{i,j}\Delta I_j, \qquad \forall 1 \le i \le N \tag{A-4}$$

The positive direction for nodal and branch currents are considered to be into and out of the corresponding node, respectively. The superimposed sending- and receiving-end current of a transmission line can be obtained based on the superimposed voltages at its two ends. The superscript *s* is used to refer to the corresponding sequence circuit and takes a value of "*z*", "*p*" or "*n*" for the zero- positive- and negative-sequence circuits, respectively. If the superimposed current of the sending-end of a line *u*-*v* with the length $l_{uv}$ in the sequence circuit *s* is denoted by $\Delta J_{uv}^{s}$, then

$$\Delta J_{uv}^{s} = \frac{\Delta V_u^s}{z_{uw}^{c,s}} \tanh\left(\frac{\gamma_{uv}^s l_{uv}}{2}\right) + \frac{\Delta V_u^s - \Delta V_w^s}{z_{uw}^{c,s} \sinh\left(\gamma_{uv}^s l_{uv}\right)} \tag{A-5}$$

where $z_{uv}^{c,s}$ and $\gamma_{uv}^{s}$ denote the characteristic impedance and propagation constant of the line *u*-*v* in the sequence circuit *s*. Substituting for the superimposed voltages of (A-5) from (A-4) yields

$$\Delta J_{uv}^{s} = \sum_{q=1}^{N} C_{uv,q}^{s} \Delta I_q^s \tag{A-6}$$

where the coefficient $C_{uv,q}^{s}$ is obtained from [21]:

$$C_{uv,q}^{s} = \frac{Z_{u,q}^{s}}{z_{uv}^{c,s} \tanh(\gamma_{uv}^{s} L_{uv})} - \frac{Z_{v,q}^{s}}{z_{uv}^{c,s} \sinh(\gamma_{uv}^{s} L_{uv})} \tag{A-7}$$

Equation (A-6) gives the superimposed current of the transmission line *u*-*v* in terms of superimposed nodal current injections in the power system.

## Appendix B: Correctness of the Solution

Let us consider an LoG event at bus *k*. Measurements are assumed to be error-free. This means the following equations derived based on KVL and KCL all hold:

$$\begin{bmatrix} h_1 \\ \vdots \\ h_n \end{bmatrix} \Delta I_k = \begin{bmatrix} m_1 \\ \vdots \\ m_n \end{bmatrix} \tag{B-1}$$

In other words, (B-1) is consistent and has an exact solution, i.e. the superimposed current injection at bus *k*. Therefore, the least-squares method gives the exact solution of this system of equations with zero *SoSR* [31]. Let us construct the system of equations for another candidate location, say bus *q*, which is not the event location. For distinction, the coefficient vector quantities derived for this candidate location are marked by the prime sign. Hence,

$$\begin{bmatrix} h_1' \\ \vdots \\ h_n' \end{bmatrix} \Delta I_q = \begin{bmatrix} m_1 \\ \vdots \\ m_n \end{bmatrix} \tag{B-2}$$

It can be easily confirmed that (B-2) will have an exact solution with the given set of measurements, only and only if:

$$\frac{h_1'}{h_1} = \frac{h_2'}{h_2} = \cdots = \frac{h_n'}{h_n} \tag{B-3}$$

Otherwise, (B-2) is not solvable and the least-squares method provides merely an approximate solution to it, hence a non-zero *SoSR* [31]. It should be mentioned that (B-3) is highly unlikely to hold true for any two PMUs on the IEEE 39-bus test system. This means that for no LoG event the true LoG location will be mistaken with another candidate location, using the data of more than one PMU.

## Appendix C: Real-Time Computation Burden

The vector of measurement residuals, denoted by $\boldsymbol{r}$, for a linear system of equations with the general form (3) can be calculated from [23]

$$\boldsymbol{r} = \boldsymbol{m} - \hat{\boldsymbol{m}} = \boldsymbol{S}\boldsymbol{m} \tag{C-1}$$

where

$$\boldsymbol{S} = \boldsymbol{I} - \boldsymbol{h}(\boldsymbol{h}^*\boldsymbol{R}^{-1}\boldsymbol{h})^{-1}\boldsymbol{h}^*\boldsymbol{R}^{-1} \tag{C-2}$$

The matrix $\boldsymbol{S}$ is called the residual sensitivity matrix as it represents the sensitivity of measurement residuals to the measurement errors. Hence, the scalar *SoSR* presented by (5) can be readily obtained from

$$SoSR = \boldsymbol{m}^*\boldsymbol{S}^*\boldsymbol{S}\boldsymbol{m} \tag{C-3}$$

The product $\boldsymbol{S}^*\boldsymbol{S}$ can be calculated in advance based on the bus impedance matrix of the system and saved in memory. It follows that evaluating the *SoSR* index for each candidate location incurs $n(n+1)$ multiplications plus $(n+1)(n-1)$ additions of complex numbers, where *n* refers to the number of PMU measurements (the size of the vector $\boldsymbol{m}$). This for 500 measurements in a large-scale power system will not exceed 0.2 ms using MATLAB on a 2.8 GHz processor with 8 GB of RAM. The calculation of *SoSR* for each location is completely independent of others. This provides the possibility of reducing the computational burden to that required for computing a single *SoSR* with proper parallelization on hardware/software level, if required.

## Appendix D: Partial Generating Unit Outages

The superimposed circuit shown in Fig. D1 is associated with an LoG event at a bus *k* in which *l* out of *u* generating units are disconnected. The remaining generating units are represented by their equivalent reactance. The outage of *l* generating units is equivalent to losing a portion of pre-event current injections represented by a suitable current source in the superimposed circuit. The relation between the superimposed current $\Delta I_k$ and the sudden current injection

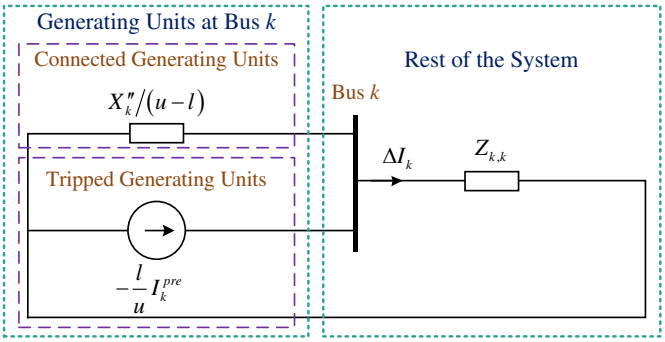


Fig. D1. Positive-sequence superimposed circuit after the outage of $l$ generating units at bus $k$.

drop due to the outage of $l$ generating units can be obtained using the current division rule as follows

$$\Delta I_k = -\frac{X_k''}{(u-l)Z_{k,k}+X_k''}\times\frac{l}{u}I_k^{pre} \tag{D-1}$$

Manipulating (B-1), the unknown variable $l$ can be expressed in terms of the other variables as below

$$l = \frac{uZ_{k,k}+X_k''}{uZ_{k,k}-X_k''\boldsymbol{\alpha}^{-1}}u = \left|\frac{uZ_{k,k}+X_k''}{uZ_{k,k}+X_k''\alpha^{-1}}\right|u \tag{D-2}$$

where the complex number $\boldsymbol{\alpha}$ denotes the ratio between $\Delta I_k$ and $I_k^{pre}$. The phase angle of $\boldsymbol{\alpha}$ will be exactly equal to $\pi$ in the case of the outage of all generating units at bus $k$. For partial outages, the phase angle of $\boldsymbol{\alpha}$ would lie quite close to $\pi$ due to the inductive nature of the Thevenin impedance at different buses in the power system. To ease the calculations, $\boldsymbol{\alpha}$ can be approximated by the ratio between $|\Delta\hat{I}_k|$ and $|I_k^{pre}|$, denoted by the scalar $\alpha$, with a negative sign. Having obtained the number of tripped generating units from (D-2), the LoG event size can be formulated as follows

$$\Delta P = \frac{lP_k^{pre}}{u} = \left|\frac{uZ_{k,k}+X_k''}{uZ_{k,k}+X_k''\alpha^{-1}}\right|P_k^{pre} \tag{D-3}$$

which is the expression given in (7).

## REFERENCES


[1] National Grid ESO, "Interim Report into the Low Frequency Demand Disconnection (LFDD) following Generator Trips and Frequency Excursion on 9 Aug 2019", 2019.

[2] S. Azizi, *et al.*, "Development and tests of new protection solutions when reaching 100% PE penetration," EU H2020 MIGRATE Project, Deliverable 4.3, Dec. 2018.

[3] P. M. Anderson, *Power System Protection*. New York: IEEE Press, 1999.

[4] S. H. Horowitz and A. G. Phadke, *Power System Relaying*, 3rd ed. John Wiley & Sons, 2008.

[5] V. Terzija, "Adaptive underfrequency load shedding based on the magnitude of the disturbance estimation," *IEEE Trans. Power Syst.*, vol. 21, no. 3, pp. 1260–1266, Aug. 2006.

[6] U. Rudez and R. Mihalic, "Monitoring the first frequency derivative to improve adaptive underfrequency load-shedding schemes," *IEEE Trans. Power Syst.*, vol. 26, no. 2, pp. 839–846, May 2011.

[7] U. Rudez and R. Mihalic, "Analysis of underfrequency load shedding using a frequency gradient," *IEEE Trans. Power Del.*, vol. 26, no. 2, pp. 565–575, Apr. 2011.

[8] R. Azizipanah-Abarghooee, M. Malekpour, M. Paolone, and V. Terzija, "A new approach to the on-line estimation of the loss of generation size in power systems," *IEEE Trans. Power Syst.*, vol. 34, no. 3, pp. 2103–2113, May 2019.

[9] P. M. Ashton, C. S. Saunders, G. A. Taylor, A. M. Carter, and M. E. Bradley, "Inertia estimation of the GB power system using synchrophasor measurements," *IEEE Trans. Power Syst.*, vol. 30, no. 2, pp. 701–709, Mar. 2015.

[10] P. Wall and V. Terzija, "Simultaneous estimation of the time of disturbance and inertia in power systems," *IEEE Trans. Power Del.*, vol. 29, no. 4, pp. 2018–2031, Aug. 2014.

[11] J. Schiffer, P. Aristidou, R. Ortega, "Online estimation of power system inertia using dynamic regressor extension and mixing," *IEEE Trans. Power Syst.*, vol. 34, no. 6, pp. 4993–5001, Nov. 2019.

[12] K. Tuttelberg, J. Kilter, D. Wilson, and K. Uhlen, "Estimation of power system inertia from ambient wide-area measurements," *IEEE Trans. Power Syst.*, vol. 33, no. 6, pp. 7249–7257, Nov. 2018.

[13] A. Derviškadić, Y. Zuo, G. Frigo, and M. Paolone, "Underfrequency load shedding based on PMU estimates of frequency and ROCOF," *2018 IEEE PES Innovative Smart Grid Technologies Conference Europe (ISGT-Europe)*, Sarajevo, 2018, pp. 1-6.

[14] G. Frigo, A. Derviškadić, Y. Zuo and M. Paolone, "PMU-based RoCoF measurements: Uncertainty limits and metrological significance in power system applications," *IEEE Trans. on Instrum. and Meas.*, vol. 68, no. 10, pp. 3810–3822, Oct. 2019.

[15] Y. Zhang, *et al.*, "Wide-area frequency monitoring network (FNET) architecture and applications," *IEEE Trans. Smart Grid*, vol. 1, no. 2, pp. 159–167, Sep. 2010.

[16] W. Li, J. Tang, J. Ma, and Y. Liu, "Online detection of start time and location for hypocenter in north America power grid," *IEEE Trans. on Smart Grid*, vol. 1, no. 3, pp. 253-260, Dec. 2010.

[17] H. X. Zhang, F. Shi, Y. T. Liu, and V. Terzija, "Adaptive online disturbance location considering anisotropy of frequency propagation speeds," *IEEE Trans. Power Syst.*, vol. 31, no. 2, pp. 931–941, Mar. 2016.

[18] N. Shams, P. Wall, V. Terzija, "Active power imbalance detection, size and location estimation using limited PMU measurements," *IEEE Trans. Power Syst.*, vol. 34, no. 2, pp. 1260–1266, Mar. 2019.

[19] D. Kim, A. White and Y. Shin, "PMU-based event localization technique for wide-area power system," *IEEE Trans. Power Syst.*, vol. 33, no. 6, pp. 5875–5883, Nov. 2018.

[20] N. D. Tleis, *Power Systems Modeling and Fault Analysis: Theory and Practice*. 7th ed., Oxford, UK: Newnes, 2008.

[21] S. Azizi and M. Sanaye-Pasand, "From available synchrophasor data to short-circuit fault identity: Formulation and feasibility analysis," *IEEE Trans. Power Syst.*, vol. 32, no. 3, pp. 2062-2071, May 2017.

[22] Desoer and E. S. Kuh, *Basic Circuit Theory*, New Delhi: Tata McGraw-Hill, 2009.

[23] A. Abur, and A. G. Exposito, *Power System State Estimation: Theory and Implementation*, Marcel Dekker, Inc., 2004.

[24] A. S. Dobakhshari, "Wide-area fault location of transmission lines by hybrid synchronized/unsynchronized voltage measurements," *IEEE Trans. Smart Grid*, vol. 9, no. 3, pp. 1869–1877, May 2018.

[25] W. Yao, *et al.*, "Impact of GPS signal loss and its mitigation in power system synchronized measurement devices," *IEEE Trans. Smart Grid*, vol. 9, no. 2, pp. 1141-1149, Mar. 2016.

[26] R. D. Zimmerman, C. E. Murillo-Sanchez, and D. Gan, "MATPOWER, a MATLAB Power System Simulation Package". ver. 3.2, 2007. [Online]. Available: http://www.pserc.cornell.edu/matpower/.

[27] S. Azizi, A. S. Dobakhshari, S. A. N. Sarmadi, and A. M. Ranjbar, "Optimal PMU placement by an equivalent linear formulation for exhaustive search," *IEEE Trans. Smart Grid*, vol. 3, no. 1, pp. 174–182, Mar. 2012.

[28] F. C. Schweppe and J. Wildes. "Power system static-state estimation, Part I: Exact model." *IEEE Trans. on Power Apparatus and system*, vol. Pas-89, no. 1, Jan. 1970.

[29] *IEEE Standard for Synchrophasor Measurements for Power Systems*, IEEE Std. C37.118.1-2011, 2011.

[30] V. Terzija *et al.*, "Wide-area monitoring, protection, and control of future electric power networks," *Proc. IEEE*, vol. 99, no. 1, pp. 80–93, Jan. 2011.

[31] *IEEE Standard* for Synchrophasor Data Transfer for Power Systems, IEEE Std. C37.118.2-2011, 2011.

[32] C. D. Meyer, *Matrix Analysis and Applied Linear Algebra*, SIAM, 2001.